

Constant Chamber Pressure Throttling of an Expansion-Deflection Nozzle

CHARLES J. SCHORR*

Textron's Bell Aerospace Company, Buffalo, N. Y.

Thrust throttling at constant chamber pressure is desirable for certain advanced engine applications. An expansion-deflection (E-D) nozzle is by its very nature altitude-compensating and throttleable. Additionally, the chamber pressure, P_c , can be maintained constant with pintle axial displacement. A study was conducted to examine the effect of throttling an E-D nozzle on nozzle performance. The analysis used the two-dimensional axisymmetric method of characteristics to calculate nozzle wall static pressure and nozzle thrust. The experimental program consisted of cold flow testing and engine testing. Using the cold-flow data (measured net thrust and chamber pressure), nozzle thrust coefficients were calculated. The effect of throttling on throat discharge coefficient and the effect of open and closed wakes on plug base pressure were studied. Test variables included throat area, nozzle pressure ratios, and throat flow angle. Analytical and experimental agreement was good. Calculated static pressure variations along the nozzle contour were in good agreement with those experimentally measured.

Nomenclature

A, A^*	= area and nozzle throat area, respectively
C_f	= measured nozzle thrust coefficient
C_{f1-D}	= one-dimensional optimum thrust coefficient
D_e	= nozzle exit diameter
F	= measured thrust
G	= throat gap
H	= water depth; H_0 at stagnation condition
K	= constant, $K = K(\gamma, M)$, used in hydraulic analogy
L	= nozzle length
P_a, P_w	= ambient and wall static pressures, respectively
P_c, P_0	= chamber and stagnation pressures, respectively
R_c	= nozzle throat radius of curvature
R_p	= pintle tip radius
R_t	= average radius at nozzle throat
X	= axial station in nozzle
γ	= specific heat ratio
ϵ	= nozzle area ratio
θ	= flow angle at throat

Introduction

THE expansion-deflection (E-D)-nozzle is one type which has several desirable characteristics^{1,2} for applications such as tactical missiles or boosters: throttleability, a reasonable throat gap when compared to other throat throttling engines such as plug and aero-spike nozzles, and altitude-compensation capability for good performance over a range of operational altitudes. Its central plug deflects the combustion products onto the nozzle wall or shroud. The combustion gases are turned by the shroud, causing high local wall static pressures. In addition, the nozzle generally operates with a freestream surface at the edge of the wake behind the central plug (or pintle). The presence of this free surface and the deflection of the combustion gases by the nozzle shroud causes P_w along the shroud to vary; it does not gradually drop off to ambient pressure P_a at the nozzle exit, as is the case with a deLaval nozzle, but rather could be cyclic,

as a function of P_a . This is the result of a pressure wave being deflected from the stream surface, etc.

The presence of freestream significantly contributes to what is called "nozzle altitude compensation." At the design altitude of the nozzle, the majority of the gas flow is axial at the nozzle exit and the freestream surface is parallel with the engine centerline. This permits as much of the flow momentum as possible to be effectively converted to thrust. During throttling, the position of the freestream will change to maintain an expansion ratio where the exit pressure is equal to P_a . The same freestream variation will occur as P_a changes while traversing the operational altitude range. This nozzle characteristic permits more effective thrust to be produced than would be the case with a deLaval nozzle which cannot efficiently be throat-area-throttled and whose nozzle performance drops significantly with altitude changes. There are, of course, potential problem areas with an E-D nozzle design, such as thermal management, plug cooling, materials, and throttle control systems.

This paper describes results from an applied research program undertaken to determine the effect of E-D nozzle design parameters on nozzle performance for constant-chamber-pressure throttling. Investigations centered about analysis, cold flow testing of two- and three-dimensional models with air and water, and correlations of the cold flow data with the hot firing data.

Theoretical Analysis

The wall of an E-D nozzle (Fig. 1) can be designed to yield an exit flow similar to that of a conventional nozzle, since the expansion of the exhaust gases occurs about a simple corner. Because of the separated flow region behind the plug, analysis of the flowfield becomes radically different and more difficult than for the full flowing conical or bell nozzle.

To design an E-D nozzle which would produce the maximum thrust for a given length for known γ , P_c , geometry, and flow in the immediate vicinity of the throat, the two-dimensional axisymmetric method of characteristics is used to develop a flowfield downstream from the throat. Also, a right-running characteristic (RRC) can be drawn emanating downstream and starting from the left side of the start line. Many reference books, such as Shapiro,³ contain good technical dis-

Received May 15, 1969; presented as Paper 69-435 at the AIAA 5th Propulsion Joint Specialist Conference, U.S. Air Force Academy, Colo., June 9-13, 1969; revision received February 13, 1970.

* Research Scientist, Propellants and Combustion Technology. Member AIAA.

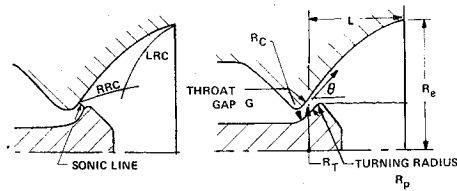


Fig. 1 E-D nozzle nomenclature.

cussions of the characteristic and compatibility equations which together comprise the method of characteristics. The calculus of variations can now be used, in addition to the fluid dynamic equations, to describe a family of left-running characteristics (LRC) emanating from various points on the right-running characteristic. The calculus of variations is a mathematical technique by which a function can be maximized subject to certain constraints. Rao⁴ uses this method to formulate a system of equations that will define a nozzle contour that yields maximum thrust for a given length under the restriction of constant flow rate by using the continuity equation for steady-state flow. Each LRC would define a different back pressure; therefore, for the ambient pressure of interest, the LRC and the exit point are defined by using the aforementioned continuity equation. However, the location where the expansion about the plug stops is quite difficult to determine. On conventional aerodynamic surfaces, the pressure at which separation occurs has been measured by enumerable investigators; in this case, the separation point of a supersonic gas stream expanding rapidly about a circular plug was obtained experimentally using base pressure measurements taken during cold flow tests described in a later section. Now, using the method of characteristics but in a backward direction from the right and the left characteristics of interest, both having been previously defined, the complete nozzle flowfield can be developed. The next step involves placing a streamline through the initial point which would be at the left end of the start line and culminating in the exit point of the nozzle (which is the same as the end of the LRC). This streamline is by definition shock-free and therefore represents the locus of points which would be a nozzle contour by the calculus of variations. This contour is the shortest one that will yield the delivered thrust.

Whereas in general the flowfield is computed using the two characteristic equations and the two compatibility equations to solve for the four unknowns of axial and radial coordinates, Mach number and flow angle, a modification is needed near the free surface between the expanding exhaust gas and the central region. Here, no left running characteristics exist, and so two additional relations are needed. Constant static

Table 1 Summary of design nozzle evaluated

Nozzle	P_a	R_t , in.	L , in.	D_e , in.	C_f/C_f noz. 1
1	14.7	1.87	3.6	8.3	1.00
2	6.7	1.87	7.7	9.5	1.03
3	14.7	1.56	4.1	8.2	1.02
4	6.7	1.56	8.1	9.4	1.05

($\theta = 75^\circ$, $R_p = 0.18$ in., $G = 0.288$ in.)

pressure, which implies a constant Mach number on the free surface supplies one of the equations, while modifying a compatibility equation to apply to a streamline (which the free surface is) produces the other equation.

As part of the computer program, P_w 's are calculated at various locations along this nozzle contour, and $P_w dA$ is integrated to produce a predicted thrust coefficient C_f which will be maximum for the nozzle length and P_a under consideration. Off-design performance (various throttle positions and P_a 's) may also be calculated. For this study, specific heat ratio γ , flow angle at the throat θ , plug tip radius of curvature R_p , throat gap G , and P_a were the parameters varied.

The effect of γ is shown in Fig. 2 for $G = 0.24$ in. and $R_p = 0.12$ in. These nozzle contours show a trend of increasing radius and length with increasing γ , a conclusion also reached by other investigators⁵ for bell nozzles. However, for any given length, a higher C_f is calculated for a γ of 1.2 than a γ of either 1.174 or 1.4. Although the nozzle area is largest for $\gamma = 1.4$, the P_w is smaller; thus, it is not surprising that a maximum C_f occurs at some intermediate γ .

The throat area of an E-D nozzle can be expressed as $A^* = 2\pi R_T G$. Therefore, for a given A^* , which is generally a design input, various G 's can be considered. Fig. 3 shows that performance is not very dependent on G , but that the gap of 0.288 in. yielded maximum performance.

Figure 4 shows that, in the range 0.06–0.18 in., R_p does not affect theoretical C_f . Other considerations showed that performance dropped off for the lower θ 's (45° and 60°), but there was very little difference in performance when the angle was 75° or 90° .

On the basis of the parametric study, the following design parameters were selected for further study: $\theta = 75^\circ$, $R_p = 0.18$ in., and $G = 0.288$ in. The effect of P_a was now considered by designing four nozzles, two at 14.7 psi back pressure and two at 6.7 psi back pressure, for R_t 's of 1.87 and 1.56 in. as shown in Table 1. C_f results are discussed later.

Water Table and Cold Flow Testing

The hydraulic analogy relates the frictionless two-dimensional flow of a liquid with a free surface to the flow of a compressible gas. A water table is an experimental tool utilizing the hydraulic analogy, in which water flows over a horizontal glass plate, around or through the model to be tested. Use of water tables to study rocket flows has been discussed by Adams⁶ and Schorr.⁷ The picture of flow through an E-D nozzle model in Fig. 5 shows that the flow patterns about the plug are symmetrical; there is no recirculation evident, but an apparent unexplainable flow phenomenon is occurring at the throat. The line which occurs at the minimum area of the

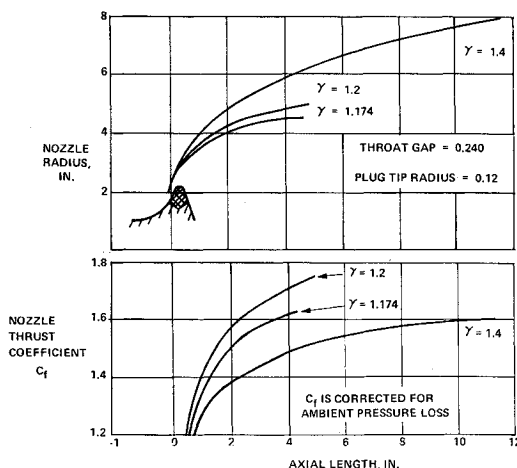


Fig. 2 Effects of specific heat on nozzle contour and performance.

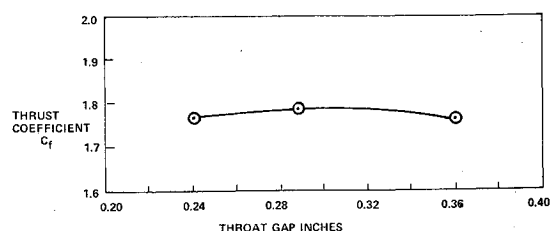


Fig. 3 Effect of throat gap on nozzle performance.

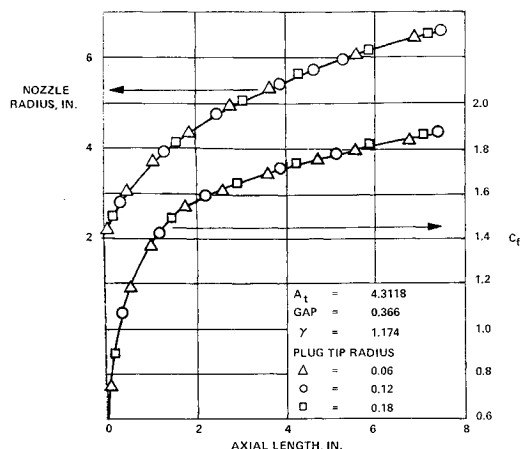


Fig. 4 Effect of plug tip radius on nozzle contour and performance.

flow regime may be considered a sonic line, but its shape is unlike that which would be analytically predicted for an E-D nozzle.⁸ Since this phenomenon is known to be real, it is under present and continuing investigation. The water table's overflow weir can be adjusted in height to simulate variations in back pressure (altitude), which change the shape of the free surface, as well as the expansion around the plug and around the nozzle exit.

A direct consequence of the hydraulic analogy is that a fundamental relationship between the pressure of the gas simulated by the analogy (P) and the height of the water being flowed in the water table (H)^{6,7} is $(P/P_0) = K(H/H_0)^2$.

A water height measuring system involving a movable datum relative to the glass base of the water table and a depth micrometer wired to a battery and voltmeter was then designed and used. The height of the micrometer off the glass bed is a known value at each point. When the depth micrometer touches the water, an electrical circuit completed through the water registers on the voltmeter. These depth measurements are taken at various stations in the chamber and along the nozzle wall to provide predictions of the nozzle wall static pressure distribution. Data on the base of the plug as well as the exit of the nozzle are also readily obtainable.

Cold-flow testing with air was done by Fluidyne Engineering Corporation under a subcontract to Bell Aerospace. One nozzle was designed with an area ratio ϵ of 53 at full thrust and θ of 90° (configuration 1, Fig. 6). After the test series, the nozzle and plug contour were modified to yield a θ of 75° (configuration 2). Configuration 3, the last to be tested, had $\theta = 75^\circ$ and $\epsilon = 35^\circ$. The other test parameters varied were the nozzle over all pressure ratio P_c/P_a (68–1300), and throat area throttling range (7–1). Measurements included P_w at 10 axial locations, P_c , back pressure, plug base pressure at five radial locations, flow rate, thrust, and throat gap. The pressures were measured, with multiple tube manometers with either mercury or silicone as the fluid. After steady state was reached, all pressures were photographically recorded on Polaroid film.

Cold Flow Results and Correlation with Analysis

The left side of Fig. 7 shows that for the full thrust tests (i.e., no throttling) with $\theta = 90^\circ$ and $\epsilon = 53$, the C_f efficiency dropped quite rapidly with decreasing pressure ratio, which represents lower altitude. A bell nozzle with a similar ϵ would perform even less efficiently; it would separate, and the effective area ratio would decrease along with the attendant separation problems. The right part of Fig. 7, showing the effect of the throttle position on the C_f efficiency, was also made using configuration 1 data but only a pressure ratio of 68, the pressure ratio that would occur for a nozzle having a 1000 psi chamber pressure and operating at sea level. It is apparent

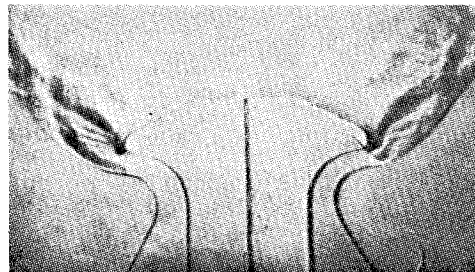


Fig. 5 Close-up of throat at maximum position: water table.

that the efficiency drops off quite rapidly with decreasing throttle position. However, it should be realized that in the low throttle position (1/7 thrust), the physical area ratio of this nozzle was on the order of 370.

Table 2 lists the major test results for the three configurations. The C_f data are not normalized and appear at first glance to be low, but caution is advised when using this table. This nozzle was designed to have a relatively large ϵ so as to operate at a large pressure ratio (1300). If this nozzle had been designed to operate at a pressure ratio of 68, the performance would have been improved significantly over that previously obtained. Operating at its design condition, this nozzle had an efficiency of 96.4%. The full-thrust efficiency of 82.7% appeared when operating at sea level. At 1/7 throttle position, this value dropped to only 52.3%; but again it should be remembered that ϵ is quite large. For example, for configuration 3, when 2.48 in. of nozzle was cut off, yielding an area ratio of 35, the sea level performance only dropped from 81.9% at full thrust to 67.7% at the 1/7 throttle position.

It is interesting to note that the nozzle contour which was designed for an operation at 90° throat flow angle did not penalize performance significantly when it was tested after being reworked to a 75° throat angle (82.7–81.9%).

The nozzle thrust coefficient, C_f , is defined as the measured thrust divided by $P_c A^*$. The C_f efficiency is this term divided by the ideal thrust developed by the same mass flow expanding to the same P_a .

$$\frac{C_f}{C_{f_{1-D}}} = \frac{F_{\text{meas}}/P_c A^*}{\{2\gamma^2/(\gamma-1)(2/(\gamma+1))^{\gamma+1/\gamma-1} \times [1 - (P_a/P_c)^{\gamma-1/\gamma}]\}^{1/2}}$$

The usual term for rocket performance is the specific impulse, I_{sp} , which is the product of the thrust coefficient C_f and the characteristic velocity C^* , a measure of propellant performance. A 10% change in C_f therefore results in a 10% change in I_{sp} .

For configuration 1 at full thrust, the discharge coefficient C_d was 0.940 as opposed to 0.994 for a conventional deLaval nozzle. However, when throttling the engine to the 1/7 point, C_d rose to 0.960. This implies that the design of the convergent or subsonic section of the nozzle is considerably more important than initially expected. Both the P_w data in the subsonic and transonic region and the C_d data indicate losses in the converging flow area of the 7/7 throat size nozzle that were reduced significantly at the more rapidly changing converging flow area at the 1/7 throat gap size. Static pres-

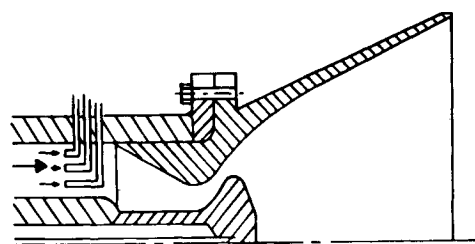


Fig. 6 Cold flow test model configuration 1 ($\theta = 90^\circ$).

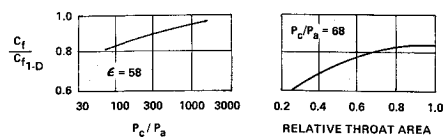


Fig. 7 Effects of design pressure ratio and throttle position on nozzle efficiency; configuration 1 ($\theta = 90^\circ$).

sure taps in the transonic region also indicated that the flow became sonic before the minimum area was reached. It is postulated that this occurred because of the rapid turning of the accelerating flow. A large percentage of flow, therefore, occupies a smaller area and causes local choking. When this sonic accelerating flow encounters the still converging area, shocks occur, causing the loss in total pressure. This loss in available energy can be minimized by properly designing the converging section.

Another interesting result involved the pressure symmetry. Three static pressure taps were located at the same axial position of the nozzle, 120° apart to determine if asymmetric flow occurred. At the larger gap settings the flow was perfectly symmetric, but at low gap settings it was not; probably due to the pintle being displaced slightly from its centerline due to manufacturing tolerances. A deviation of only 0.001 in. on a G of 0.025 in. at a R_i of 1.043 in. will result in a throat area circumferential deviation of 4%.

Figure 8 presents the nozzle wall static pressure distribution. For the full thrust position the analytical predictions are also illustrated. The pre-separation test and predicted wall static pressures were in close agreement. The post separation magnitudes of the pressures were predicted quite accurately as was the pressure decay when separation did not occur.

For the fully throttled (1/7) thrust position an analytical prediction of pressures could not be made due to a mathematical problem that occurs for very small throat gap settings. However, some interesting conclusions can be drawn. When P_w decreases below P_a as indicated by the symbol on the right-hand side of the figure, the flow ceases to expand and instead, P_w rises to a value above P_a , then expansion continues. This oscillation about the P_a point continues until the flow leaves the nozzle. This minimizes the nozzle surface area over which $P_w < P_a$ (the local drag region). The deLaval nozzle,

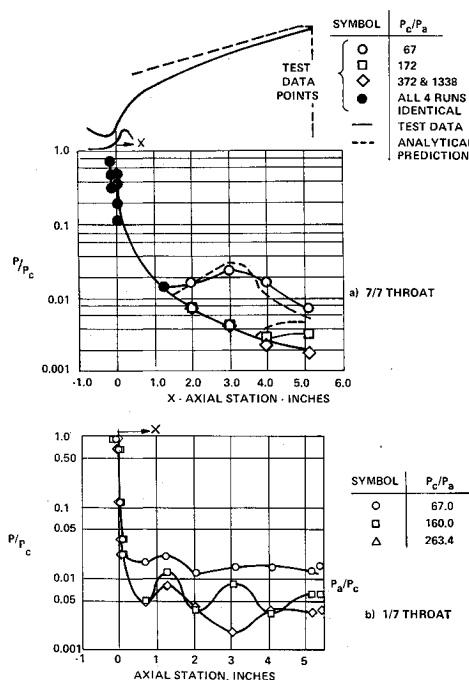


Fig. 8 Static pressure distribution for model 1.

Table 2 Tabulation of major cold flow test results

Configuration		Relative G	P_c/P_a	$\frac{C_f}{C_f 1 - D}$	C_d	
1) (90° throat)		7/7	67.1	0.827	0.943	
			172.0	0.854	0.946	
			372.2	0.932	0.940	
			1338	0.964	0.939	
		$\epsilon \frac{7}{7} = 53$	63.5	0.783	0.949	
		6/7	67.3	0.781	0.973	
		5/7	68.9	0.760	0.964	
		4/7	140.4	0.838	0.967	
			471.1	0.908	0.955	
			3/7	69.4	0.696	0.980
2) (75° throat)		7/7	63.2	0.797	0.960	
			69.7	0.552	0.960	
		$\epsilon \frac{7}{7} = 53$	67.4	0.819	0.965	
			788.4	0.940	0.962	
			1/7	69.9	0.677	0.959
	3) (75° throat, truncated shroud)	7/7	67.4	0.819	0.965	
			788.4	0.940	0.962	
			1/7	69.9	0.677	0.959

however, can over-expand to P_w as small as $P_a/3$, producing large amounts of drag.

This phenomenon can perhaps be better explained using Fig. 9. Let P_1 be the point at which the Mach line starting from where separation occurs on the plug ends on the nozzle contour. The P_w 's from the throat to P_1 are completely defined by the expansion fan. However, downstream from P_1 the flow of the exhaust gases is controlled by two boundary conditions: the nozzle wall contour and P_a . Immediately downstream from P_1 , P_w should start to increase due to the compressive turning that is occurring in that region. This occurs until Q_1 where a reflected wave coming from the free surface would reach the nozzle wall. From this point, P_w should again drop and continue in this cycle or pattern depending on how often the characteristics or Mach lines can reflect off the nozzle wall and the free surface.

E-D Nozzle Design and Firing Tests

From the foregoing results, an E-D nozzle capable of operating at 1000 psia chamber pressure was designed. The small throat radius, sea level nozzle (Table 1, nozzle 3) was selected because it yielded the best performance of the sea level designs. Consideration was given to nozzle 1, which is shorter than nozzle 3. The tradeoff in length between the two sea level designs is offset by the greater structural needs of shorter nozzle 1. The action of chamber pressure over the pintle of the smaller throat radius nozzle (nozzle 3) produces a smaller ejection load on it. Moreover, the 1.560-in. throat radius provides a smooth convergence which should minimize the friction losses of the transonic region. This part of the contour is critical since, for maximum performance, the minimum

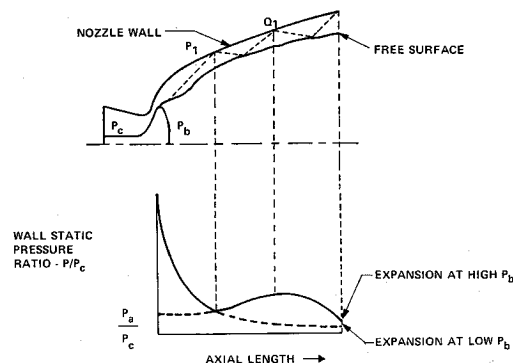


Fig. 9 E-D nozzle altitude compensation feature.

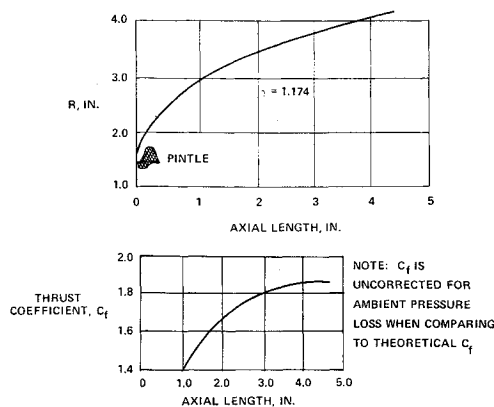


Fig. 10 Optimum contour and predicted thrust coefficient.

geometric area, A^* , must be well-defined, and flow at the throat must be directed at the proper angle. The most obvious way to do this would be to have parallel walls. However, if this were the case, the divergent area might not increase at a rapid enough rate to preclude loss-inducing shocks.

The optimum E-D nozzle contour, expanding to sea level, and its predicted performance integrated along the nozzle wall are shown in Fig. 10. The correction in predicted thrust due to the pressure forces on the plug and the throat momentum has been applied to this figure, yielding a thrust coefficient of 1.85. Correcting C_f by the ambient pressure term, $P_a/A_e/P_t A^*$, and then including three-dimensional drag losses would reduce the predicted C_f to 97.5% of theoretical at sea level. Due to the propellant combination (a fluorinated oxidizer and metallized fuel) used in the tests, two-phase and kinetic losses would be present and make up the balance of the losses.

Included in the tests of the E-D nozzles were nozzle exit pressure measurements. On three sea-level tests these pressures measured 13.9, 14.8, and 14.7 psia compared to a predicted analytical value of 14.7. The most accurate measured value resulted in a C_f of 94.5% of theoretical, which compares well with the predicted value, considering that 3% of the losses are due to the two-phase and kinetic effects.

Conclusions

1) Cold flow and firing test results corroborate analytical predictions of E-D nozzle performance and pressure profiles.

2) Firing tests have shown that high performance ($C_f = 94.5\%$ theoretical for the propellant used) is achievable with a short E-D nozzle. Higher nozzle performance would result if neat propellants were used, since two-phase losses would not occur.

3) On firing tests where nozzle exit pressure measurements were made, the nozzle generally expanded to within 1 psia of ambient pressure. This result is indicative of the altitude compensation or optimal expansion quality of the E-D nozzle (a C-D nozzle would have over-expanded to below ambient pressure, thus yielding lower performance).

4) Cold flow throttle test results revealed that significant performance gains are made when throttling at constant or near constant chamber pressure as compared to thrust throttling with no corresponding throat area change.

5) Nozzle performance at a throat angle (θ) of 90° was maximum for the E-D nozzles analyzed. However, at $\theta = 75^\circ$ the full thrust performance drop was not considered significant, particularly since the shallower throat angle was expected to be more durable in an actual engine test.

References

- ¹ Rao, G. V. R., "The E-D Nozzle," *Astronautics*, Sept. 1960, pp. 28, 29, 50, 51.
- ² Rao, G. V. R., "Analysis of a New Concept Rocket Nozzle," "Progress in Astronautics and Rocketry," Vol. 2, *Liquid Rockets and Propellants*, Academic Press, New York, 1960, pp. 669-682.
- ³ Shapiro, A. H., "The Dynamics and Thermodynamics of Compressible Fluid Flow," Vol. II, Ronald Press, New York, 1954, pp. 676-682.
- ⁴ Rao, G. V. R., "Exhaust Nozzle Contour for Optimum Thrust," *ARS Journal*, Vol. 31, 1961, pp. 614-620.
- ⁵ Ahlberg, J. H. et al., "Truncated Perfect Nozzles in Optimum Nozzle Design," *ARS Journal*, Vol. 31, 1961, pp. 614-620.
- ⁶ Adams, D. M., "Application of the Hydraulic Analogy to Axisymmetric Nonideal Compressible Gas Systems," *Journal of Spacecraft and Rockets*, Vol. 4, No. 3, March 1967, pp. 359-363.
- ⁷ Schorr, C. J., "Pressure Ratio Correction Factor When Utilizing the Hydraulic Analogy," *Journal of Spacecraft and Rockets*, Vol. 5, No. 9, Sept. 1968, pp. 1119-1120.
- ⁸ Hopkins, D. F. and Hill, D. E., "Transonic Flow in Unconventional Nozzles," *AIAA Journal*, Vol. 6, No. 5, May 1968, pp. 838-842.